Mapping Responses of Lumbar Paravertebral Muscles to Single-Pulse Cortical TMS Using High-Density Surface Electromyography

Naifu Jiang, *Member, IEEE*, Lin Wang, Zhen Huang, and Guanglin Li, *Senior Member, IEEE*

***Abstract*— Motor evoked potential (MEP), which was elicited by transcranial magnetic stimulation (TMS), has been widely used to detect corticospinal projection from TMS cortical site to trunk muscles. It can help to find the stimulation hotspot in the scalp. However, it fails to precisely describe coordinated activities of trunk muscle groups with only single-channel myoelectric signal. In this study, we aimed to use high-density surface electromyography (sEMG) to explore the effect of cortical TMS on lumbar paravertebral muscles in healthy subjects. The cortical site at 1 cm anterior and 4 cm lateral to vertex was chosen to simulate using a single-pulse TMS with different intensities and forward-bending angles. A high-density electrode array (45 channels) was placed on the surface of lumbar paravertebral muscles to record sEMG signals during a TMS experiment. MEP signals elicited by TMS were extracted from 45-channel recordings and one topographic map of the MEP amplitudes with six spatial features was constructed at each sampling point. The results showed TMS could successfully evoke an oval area with high intensity in the MEP topographic map, while this area mainly located in ipsilateral side of the TMS site. Intensity features related to the high intensity area rose significantly with TMS intensity and forward-bending angle increasing, but location features showed no change. The optimal stimulation parameters were 80% of maximum stimulator output (MSO) for TMS intensity and 30/60 degree for forward-bending angle. This study provided a potentially effective mapping tool to explore the hotspot for transcranial stimulation on trunk muscles.**

***Index Terms*— Electromyography, biomedical measurement, transcranial magnetic stimulation, motor evoked potentials, trunk muscle.**

I. Introduction

TRANSCRANIAL stimulation such as transcranial magnetic stimulation (TMS) and transcranial electrical stimulation (TES) is a potential and popular non-invasive neuromodulation technique. In the past decade, more and more studies investigated the effect of this technique on different diseases. Majority of the studies on the muscle disorder of extremities (e.g., phantom limb pain) showed good intervention effect [1], [2]. Nevertheless, with respect to the muscle disorder of trunk (e.g., low back pain), no consistent conclusion had been drawn [3]–[6]. This was probably because that the corticospinal drive to the trunk muscles is different with that to the muscles of the extremities. For trunk muscles, this drive effect was considered to have a stronger bilateral hemispherical input [7], [8]. Thus, it is significant to explore the certain relationship between the transcranial stimulation and the response of trunk muscles.

Motor evoked potential (MEP), which was elicited by TMS, from lumbar paravertebral muscles (a typical type of trunk muscles) has been widely used to detect corticospinal projection from TMS cortical site to trunk muscles. MEP signals were often recorded via surface electromyography (sEMG) electrodes during different designed movements (e.g., trunk extension, shoulder flexion, weight-lifting), while the electrodes were placed on different trunk muscles (e.g., erector spinae and rectus abdominis) [9], [10]. The variation of MEPs can reveal the law of change of corticospinal excitability. For disorder of trunk muscles such as low back pain, the amplitude of MEPs of the lumbar paravertebral muscles can be used to investigate the mechanism and physiologic effects of some novel treatments [11], [12]. Both the ipsilateral and contralateral MEPs can be found from the erector spinae [7], [8]. By employing the TMS to map the cortical representations of the lumbar paravertebral muscles, some studies even preliminarily found out the optimal site of stimulation (also called "hotspot"), situated 1 cm anterior and 4 cm lateral to the vertex, for evoking responses in the lumbar paravertebral muscles [5], [13]–[15]. However, in previous studies, researchers

Manuscript received December 1, 2020; revised March 30, 2021; accepted April 21, 2021. Date of publication April 27, 2021; date of current version May 5, 2021. This work was supported in part by the National Key Research and Development Program of China under Grant 2019YFC1710400 and Grant 2019YFC1710402, in part by the National Natural Science Foundation of China under Grant 62001463 and Grant 81927804, in part by the Guangdong Basic and Applied Basic Research Foundation under Grant 2021A1515011918, in part by the Shenzhen Science and Technology (S&T) Program under Grant SGLH20180625142402055, in part by the Shenzhen S&T Layout Project under Grant JCYJ20170818163445670, and in part by the Guangdong S&T Project under Grant 2018A030313065. *(Naifu Jiang and Lin Wang contributed equally to this work.)* This study has been approved by the Institutional Review Board. *(Corresponding author: Guanglin Li.)*

This work involved human subjects or animals in its research. Approval of all ethical and experimental procedures and protocols was granted by the Institutional Review Board.

Naifu Jiang, Lin Wang, and Guanglin Li are with the CAS Key Laboratory of Human-Machine Intelligence-Synergy Systems, Shenzhen Institute of Advanced Technology (SIAT), Chinese Academy of Sciences (CAS), Shenzhen 518055, China, also with SIAT Branch, Shenzhen Institute of Artificial Intelligence and Robotics for Society, Shenzhen 518055, China, and also with the Guangdong-HongKong-Macao Joint Laboratory of Human-Machine Intelligence-Synergy Systems, Shenzhen 518055, China (e-mail: nf.jiang@siat.ac.cn; lin.wang1@siat.ac.cn; gl.li@siat.ac.cn).

Zhen Huang is with the Panyu Central Hospital, Guangzhou 511400, China (e-mail: mishz@126.com).

Digital Object Identifier 10.1109/TNSRE.2021.3076095

primarily collected and analyzed the MEPs from one spot on the surface of muscle, using only single-channel surface electromyographic (sEMG) electrode, without taking other adjacent spots into consideration. Consequently, the coordinated activities of trunk muscles including superficial muscles and deep muscles cannot be revealed. Besides, because it is very difficult to avoid the influence of transcranial stimulation on the cortical area around the stimulation site [3], [15], the transcranial stimulation undoubtedly activates more unexpected muscles more or less. Thus, it is necessary to investigate the TMS-evoked response of all spots of lumbar paravertebral muscles rather than only one target spot. Through observing the MEPs from most muscle spots in the low back area, the effect of transcranial stimulation on the corticospinal projection can be observed more precisely and the accurate hotspot for treatment of trunk muscles' disorder may be obtained.

High-density sEMG technique provided a solution to gain all MEPs from a local area in a high resolution. For extremity muscles, there has been some studies on MEP measurement by using high-density sEMG electrodes. They measured the multi-channel MEP signals, by attaching a high-density sEMG electrodes' grid to the surface of extensor carpi radialis (ECR), extensor carpi ulnaris (ECU) and extensor digitorum communis (EDC) of the forearm [16]–[18]. The previous studies found out the topographic map of MEP amplitudes could quantify not only the temporal but also the spatial characteristics of evoked muscle activities with high resolution. These results also indicated non-targeted activated muscle (ECU and EDC) instead of targeted activated muscle (ECR) was primarily correlated to the spatial distribution of MEP topographic map under some stimulation parameters. However, for trunk muscles, there was no MEP studies based on high-density sEMG signals. Some researchers tried to collect high-density sEMG signals from back area, so as to assess the coordinated activities of different trunk muscles [19]–[21]. The extracted features from high-density sEMG signal could even be used to make a prognostic prediction of specific rehabilitation program for low back pain [22]–[24]. These results can motivate us to use high-density sEMG mapping technique to find out the corticospinal projection from transcranial stimulation to lumbar spine paraspinal muscles more comprehensively and precisely.

Therefore, this study aimed to use high-density sEMG to investigate the effect of cortical TMS on lumbar paravertebral muscles in healthy subjects. This study will provide a preliminary conclusion for the feasibility and optimal parameters to use the elicited high-density MEP mapping information to localize the hotspot precisely.

II. Methods

A. Participants

A total of twelve healthy and right-handed male participants were recruited from the local institute. With respect to the sample size, we designed it according to previously relevant hotspot-searching studies on lumbar paraspinal muscles [5], [12]–[14]. The data with more than 9 participants was found to be enough to draw an effective preliminary conclusion. Within the protocol, individuals who had history of psychiatric, neurological, implanted medical devices, or currently taking psychotropic medications were excluded. Participants' characteristics including physiological and psychological variables were recorded before the experimental process. All participants gave their written informed consent before the test and were paid for their participation. The experimental procedure was performed in accordance with the Declaration of Helsinki and was approved by the Institutional Review Board of Shenzhen Institutes of Advanced Technology, Chinese Academy of Sciences (IRB No.: SIAT-IRB-191115-H0393, November 2019).

B. High-Density sEMG Measurement

In previous studies [5], [13]–[15], in order to reduce the influence of waist girth to the statistical results, the researchers often tried to apply the identical measurement scale to localize the TMS site and sEMG electrode's position. The distance (e.g., cm) was generally used as the scale. Thus, in this study, we also used the distance scale (cm) to place the TMS coil and the high-density sEMG electrodes, so that the size of waist girth had little influence on the statistical results. In addition, the body mass index (BMI) of the recruited subjects was in an ideal range of normal weight (18.5-24.9). The High-density surface electrodes (Ag/AgCl electrode, IED $= 1.5$ cm) in a 3×15 array (45 electrodes) were attached to the skin in the low back area between the lateral edges of the torso (horizontally) and the L2-L4 level (vertically). The main lumbar paravertebral muscles are arranged into three muscular columns: lateral, the iliocostalis; intermediate, the longissimus and medial, the multifidus [25]. In order to obtain the MEP response from all lumbar paravertebral muscles, the placement of high-density sEMG electrodes covered all area of these muscles. Excluding the 45 electrodes, another one electrode was attached to the surface of sacral vertebrae as the ground (GND). In order to make the placement of the electrodes understood more easily, the detailed location of electrodes was also shown in the Fig. 1A. Before the sEMG electrodes were attached, the skin preparation for sEMG was done according to the following procedures to keep the skin impedance less than 10 kΩ: cleaning the site with alcohol wipe, shaving the electrode site (if the skin surface at the sensor location was covered with noticeable hair), and lightly ab rading the skin with fine sandpaper. The monopolar sEMG signal from 45 sEMG electrodes were differentially amplified versus the reference electrode. The sEMG signal was acquired at a sample rate of 2048 Hz and was band-filtered between 10 and 1000 Hz (REFA, TMSi International, the Netherlands). 50Hz powerline influence was removed by digital notch filters. The cardiac artifact was filtered by the independent component analysis (ICA) method.

C. TMS Intervention

Different with the MEPs of forearm muscles, MEPs of the trunk muscles are difficult to be elicited [5], [12]–[14]. In previous hotspot-searching studies on lumbar paraspinal muscles, the researchers often looked for the hotspot by

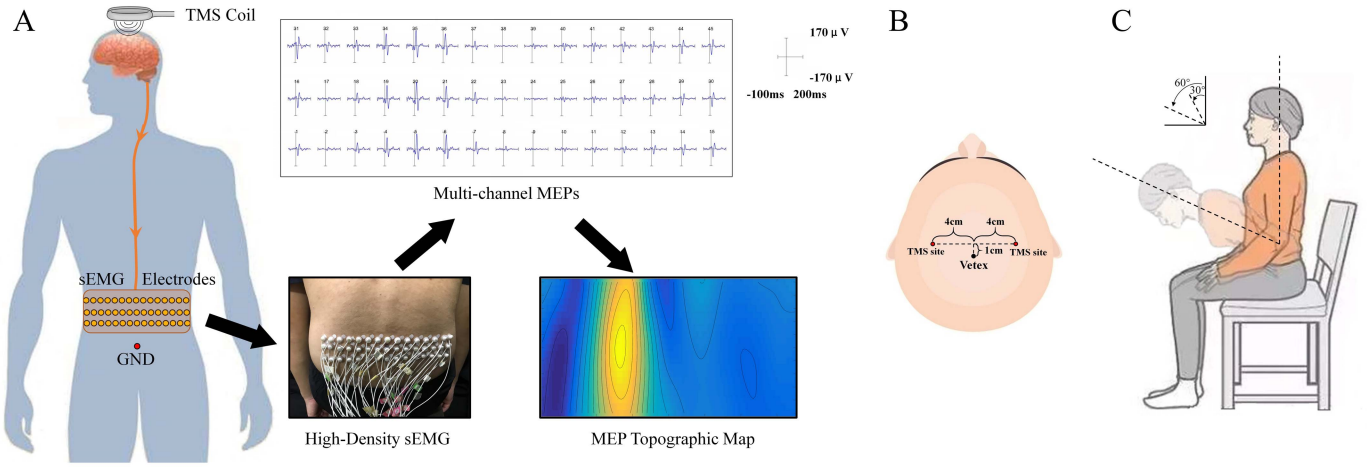

Fig. 1. Experimental procedure and data processing procedure. (A) Acquisition and processing of high-density sEMG data; (B) Location of cortical-TMS site; (C) Forward-bending angle during straight sitting.

directly using 100% of maximum stimulator output (MSO) as the TMS intensity to elicit consistent MEPs [5], [12]–[14], rather than using active motor threshold (AMT) or resting motor threshold (RMT). Besides, the use of multi-channel MEPs can lead to a different hotspot-searching process with the previous standard single-channel MEP-based process. For single-channel MEP, the AMT/RMT was often obtained from the signal of a single muscle. For multi-channel MEPs, it was difficult to find the appropriate AMT/RMT because the signals reflected the muscle synergy rather than single muscle's activity [19], [21], [22]. Thus, we did not follow the previous TMS standard process.

A repetitive biphasic Magstim Rapid2 TMS system (Magstim Company, UK) was used to deliver the stimuli to motor cortex (Fig. 1A). The stimuli were delivered by using single pulse mode with a 70mm figure-of-eight coil. In order to elicit the MEPs more easily, 45° from the sagittal plane was chosen as the most appropriate oriented angle for coil handle. The stimulation site was located 1 cm anterior and 4 cm lateral to the vertex (Fig. 1B), because it might be the optimal site, displayed in previous studies, for evoking responses in the lumbar spine paravertebral (LP) muscles [5], [12]–[14]. During the stimulation, the participant was seated comfortably in a chair with the back straight and arm falling.

Multi-channel MEPs were extracted from sEMG signals by using multi-channel sEMG electrodes. Two types of stimulation parameters (TMS intensity and forward-bending angle) were simultaneously set to elicit multi-channel MEPs. According to the previous studies [5], [8], [12]–[14], [26]–[31] and taking the risk to induce epilepsy with long experimental duration into consideration, the TMS intensity was set as 60%, 80%, or 100% of maximum stimulator output (MSO) while the forward-bending angle was 0 degree, 30 degree, or 60 degree from vertical line in sagittal plane in a trial (Fig. 1C). Each trial consisted of six stimuli, delivered to the site with an inter-stimulus interval of 3-6 seconds, with the same stimulation parameters (TMS intensity and forward-bending angle). Participants were given 5-minutes resting period between trials, so as to minimize the potential for muscle fatigue.

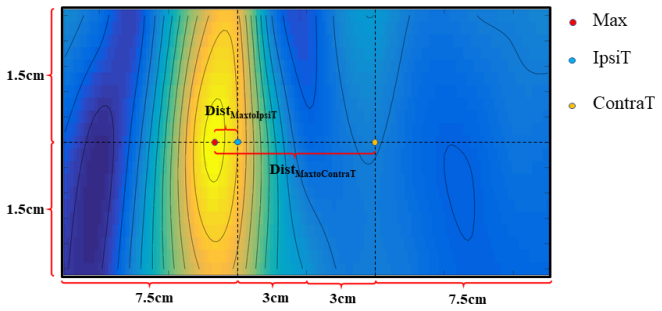

Fig. 2. Feature parameters of MEP topographic map. Peak-to-peak amplitude of the MEP (10ms-40ms following the TMS stimulation) was calculated from each channel to form the MEP topography.

D. Data Analysis

The amplitude of each MEP was calculated between the 10ms and 40ms following each stimulation. The peak-to-peak value between the onset and offset latencies of the MEP was regarded as the amplitude of the MEP. After obtaining all channels' amplitude of MEP, the method of linear cubic spline interpolation was used to estimate the amplitude of MEP among each channel. By transferring the amplitude value of MEP to corresponding color, a topographic map called MEP topographic map could be constructed (Fig. 2). The spot with the maximum amplitude value of MEP in the MEP topographic map was marked as Max. It was supposed to be in the center of the high intensity area. According to previous studies [5], [13], [14], the spot 3 cm lateral to the L3 spinous process (central spot in the topographic map) was the target LP muscle spot which showed the most response elicited by TMS on the site 1 cm anterior and 4 cm lateral to the vertex. Due to the different side of the TMS site and target LP muscle spot, the muscle spot in the ipsilateral side of the TMS site was marked as the IpsiT while that in the contralateral side was marked as the ContraT. In order to analyze the high intensity area in the MEP topographic map, five feature parameters named MEPMax, MEPIpsiT, MEPContraT, DistMaxtoIpsiT, and DistMaxtoContraT were extracted. MEPMax was the amplitude value of MEP of the Max spot. MEPIpsiT and

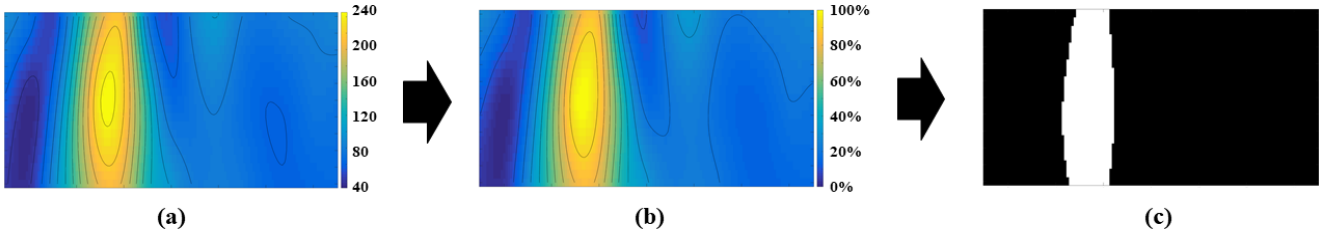

Fig. 3. Processing of MEP topographic map to extract the feature parameter named Relative Area. (a) original MEP topographic map. (b) normalized MEP topographic map. (c) binary MEP topographic map.

MEPContraT were respectively the amplitude value of MEP of the IpsiT spot and ContraT spot. DistMaxtoIpsiT and DistMaxtoContraT were the distance from the Max spot to the target spot (IpsiT spot or ContraT spot). These five parameters were mainly used to describe the intensity feature and location feature of the high intensity area.

Except the intensity and location feature, the density feature of the high intensity area in the MEP topographic map should also be extracted. By adjusting the elements' range of the topographic map between the maximum amplitude of MEP and minimum amplitude of MEP, the original MEP topographic map (Fig. 3a) was normalized. Then by setting the threshold value, the normalized MEP topographic map (Fig. 3b) could be transferred to the binary MEP topographic map (Fig. 3c). In this study, the threshold value was set as 70%. In the Fig. 3c, the proportion of the white area with respect to the entire topographic map was the sixth feature parameter, which was named Relative Area, so as to measure the density feature of the high intensity area.

E. Statistical Analysis

SPSS 19.0 (IBM, Armonk, NY, USA) was applied to conduct all statistical analyses. The demographic variables and clinical characteristics variables were compared with χ^2 test and independent T test. In order to obtain the optimal MEP topographic feature parameters for precise activation of LP muscle, we applied a two-way analysis of variance (ANOVA) to evaluate the influence of the TMS intensity (60% vs. 80% vs. 100% of the MSO) and forward-bending angle (0 degree vs. 30 degree vs. 60 degree) on each MEP topographic feature parameter. Partial eta squared (η_p^2) was calculated as a measure of the effect size. Mean square error (MSe) was also presented. Post-hoc multiple comparisons were performed with Bonferroni correction. Two-tailed p values were set at 0.05.

III. Results

With three participants dropped out, the remaining nine participants accomplished all experiments. The demographic characteristics and clinical characteristics were shown in the Table I. With respect to adverse effects, only one participant reported a severe dizziness during stimulation, but no one withdrew the experiment. No unexpected adverse events (e.g., seizure, headache) were observed during and after intervention.

TABLE I
Participant Characteristics

Characteristics	Mean ± Standard Deviation
Age (years)	24.58 ± 1.78
Weight (kg)	65.58 ± 6.05
Height (cm)	174.83 ± 5.17
BMI (kg/m2)	21.46 ± 1.88

BMI = Body Mass Index.

A. MEP Topographic Maps During Different TMS Intensity and Forward-Bending Angle

In order to compare the MEP topographic maps more conveniently, the normalized MEP topographic maps (Fig. 4, Fig. 5) were calculated and applied. With shown in Fig 4 and Fig. 5, most high intensity area (value larger than 70%), featured with an oval boundary, were distributed around one spot in the topographic map. Through visual inspection, the vertical distance from this spot to the L3 horizontal line was smaller than that to the L2 horizontal line and to the L4 horizontal line in most topographic maps. It indicated this spot normally located around the horizonal line of the L3 spinous process. In comparison of the results between left-side TMS and right-side TMS, a similar distributions of high intensity area were found. The high intensity area was ipsilateral with the TMS no matter which side of TMS. In Fig. 4 and Fig. 5, the location of the maximum response in MEP topographic maps showed some difference with different conditions. It did not mean different muscles were activated. It meant the synergy of muscle groups which was displayed by high-density sEMG signals were differently activated. Because the locations of lumbar paravertebral muscles are different, the change of muscle synergy (weight value of each muscle's activity) can lead to the shifting of the high intensity area in the MEP topographic map.

B. Comparison of Feature Parameters of MEP Topographic Maps During Different TMS Intensity and Forward-Bending Angle

All feature parameters of MEP topographic maps during different TMS intensity and forward-bending angle were displayed in the Fig. 6.

For Relative Area, the two-way ANOVA revealed a significant main effect of forward-bending angle [$F(2, 152) = 12.260$; $p < 0.001$; $\eta_p^2 = 0.139$]. Post-hoc comparisons showed

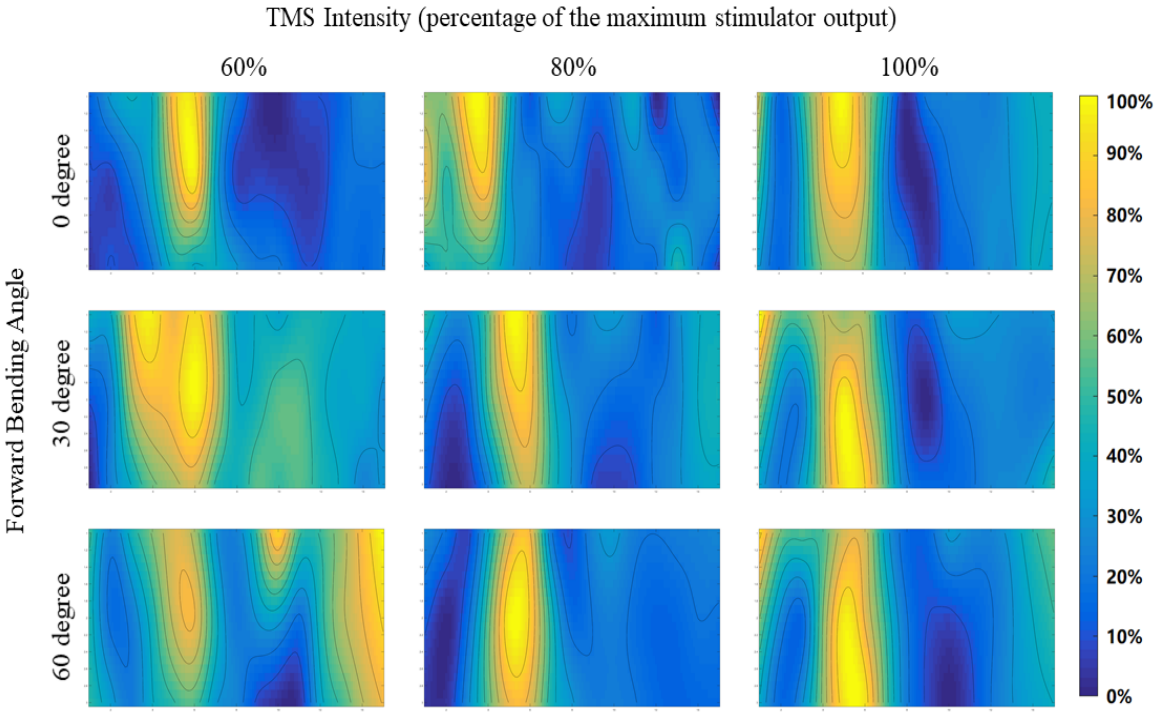

Fig. 4. Normalized MEP topographic maps while left-side TMS (one sample participant).

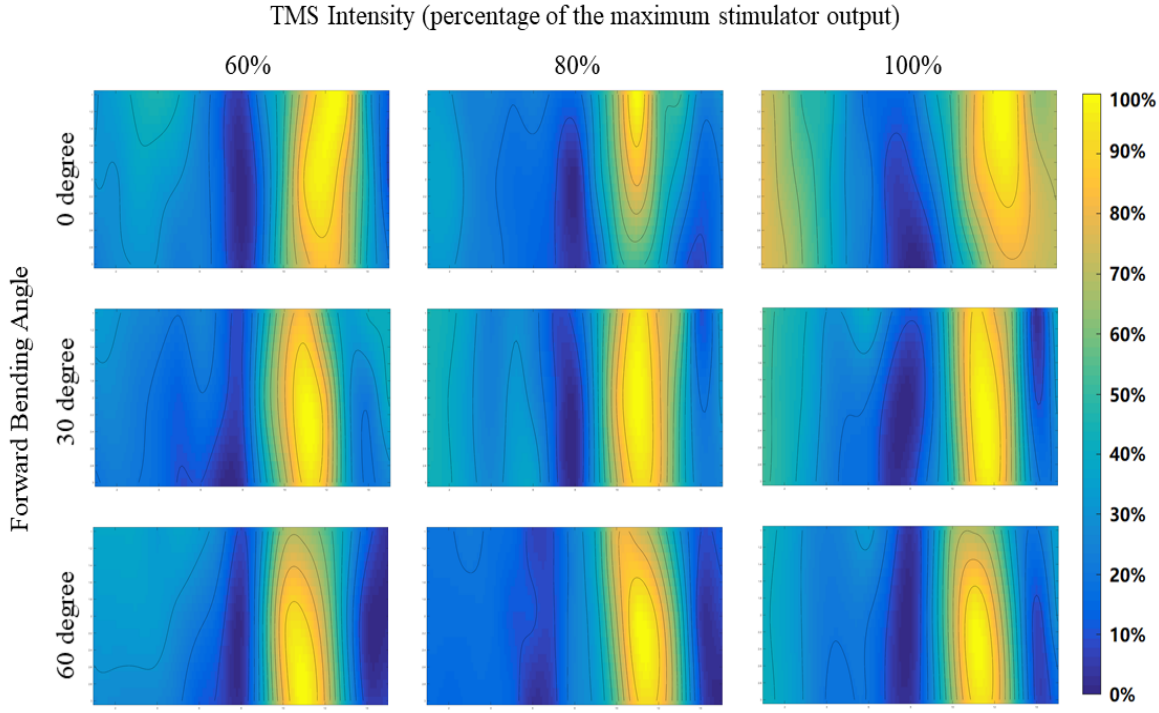

Fig. 5. Normalized MEP topographic maps while right-side TMS (one sample participant).

that Relative Area during 0 degree was significantly smaller than that during 30 degree ($p < 0.001$) and that during 60 degree ($p < 0.001$). There was no significance on interaction effect and main effect of TMS Intensity.

For MEPMax, the two-way repeated measures ANOVA revealed a significant interaction effect between TMS Intensity and forward-bending angle [$F(4, 152) = 6.082$; $p < 0.001$; $\eta_p^2 = 0.138$]. Meanwhile, main effects of TMS Intensity [$F(2, 152) = 26.175$; $p < 0.001$; $\eta_p^2 = 0.256$] and forward-bending angle [$F(2, 152) = 48.969$; $p < 0.001$; $\eta_p^2 = 0.392$] were both significant. For factor of forward-bending angle, post-hoc comparisons showed that MEPMax during 0 degree,

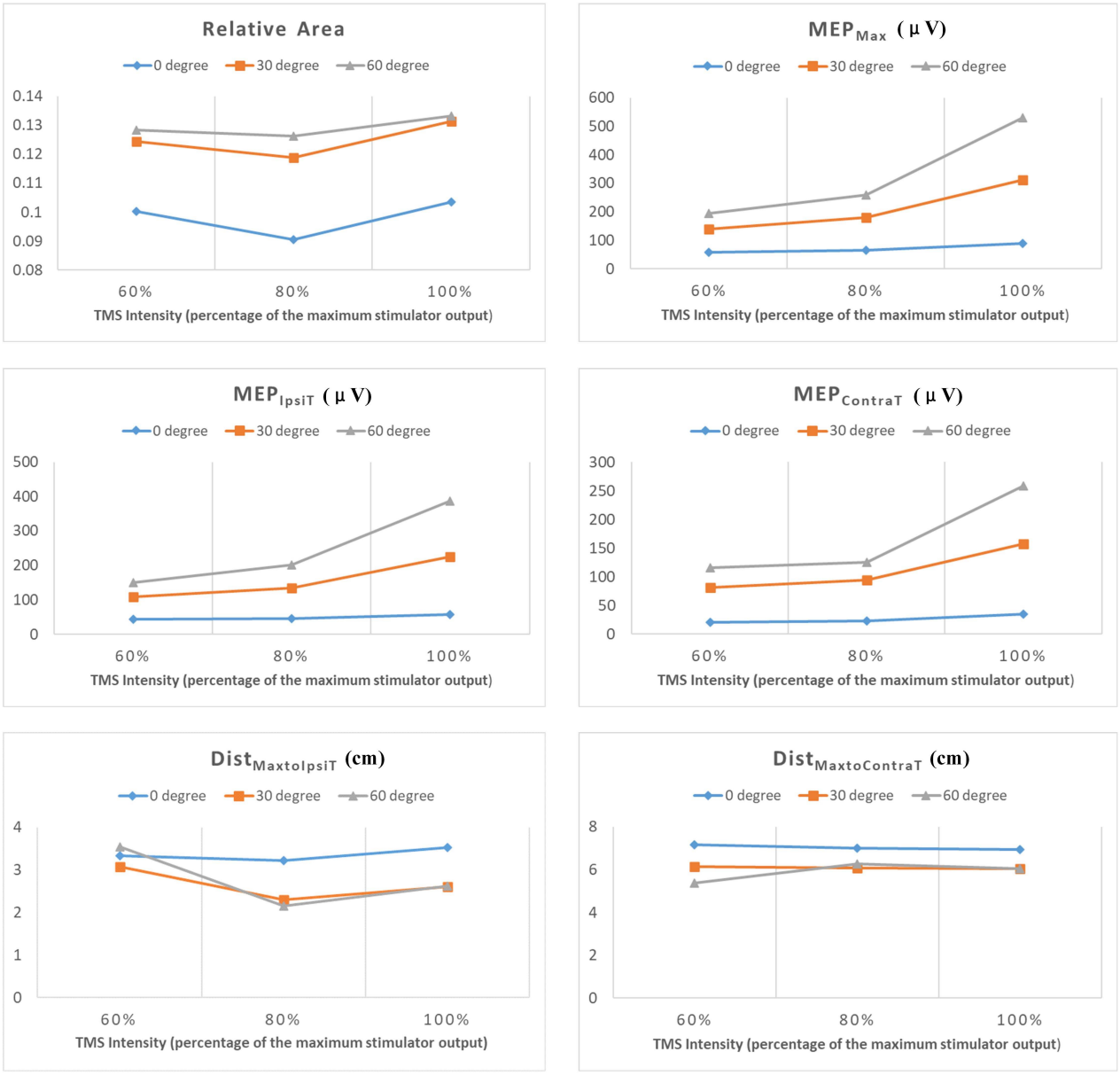

Fig. 6. Feature parameters of MEP topographic maps during different TMS intensity and forward-bending angle. IpsiT means the target muscle spot in the ipsilateral side of the TMS site, while ContraT means the target muscle spot in the contralateral side of the TMS site. Max means the muscle spot with the maximum amplitude value of MEP. The unit of amplitude of MEP (MEP) is μV while the unit of Distance (Dist) is cm.

30 degree and 60 degree were significantly different between each other [0 degree vs. 30 degree ($p < 0.001$); 0 degree vs. 60 degree ($p < 0.001$); 30 degree vs. 60 degree ($p < 0.001$)]. For factor of TMS Intensity, post-hoc comparisons showed that MEPMax during 100% of MSO was significantly larger than that during 60% of MSO ($p < 0.001$) and that during 80% of MSO ($p < 0.001$).

For MEPIpsiT, the two-way repeated measures ANOVA revealed a significant interaction effect between TMS Intensity and forward-bending angle [$F(4, 152) = 7.270$; $p < 0.001$; $\eta_p^2 = 0.161$]. Meanwhile, main effects of TMS Intensity [$F(2, 152) = 27.014$; $p < 0.001$; $\eta_p^2 = 0.262$] and forward-bending angle [$F(2, 152) = 64.120$; $p < 0.001$; $\eta_p^2 = 0.458$] were both significant. For factor of forward-bending angle, post-hoc comparisons showed that MEPIpsiT during 0 degree, 30 degree and 60 degree were significantly different between each other [0 degree vs. 30 degree ($p < 0.001$); 0 degree vs. 60 degree ($p < 0.001$); 30 degree vs. 60 degree ($p < 0.001$)]. For factor of TMS Intensity, post-hoc comparisons showed that MEPIpsiT during 100% of MSO was significantly larger than that during 60% of MSO ($p < 0.001$) and that during 80% of MSO ($p < 0.001$).

For MEPContraT, the two-way repeated measures ANOVA revealed a significant interaction effect between TMS Intensity and forward-bending angle [$F(4, 152) = 3.455$; $p = 0.010$; $\eta_p^2 = 0.083$]. Meanwhile, main effects of TMS Intensity

[F(2, 152) = 14.648; $p < 0.001$; $\eta_p^2 = 0.162$] and forward-bending angle [F(2, 152) = 40.847; $p < 0.001$; $\eta_p^2 = 0.350$] were both significant. For factor of forward-bending angle, post-hoc comparisons showed that MEPContraT during 0 degree, 30 degree and 60 degree were significantly different between each other [0 degree vs. 30 degree ($p < 0.001$); 0 degree vs. 60 degree ($p < 0.001$); 30 degree vs. 60 degree ($p = 0.003$)]. For factor of TMS Intensity, post-hoc comparisons showed that MEPContraT during 100% of MSO was significantly larger than that during 60% of MSO ($p < 0.001$) and that during 80% of MSO ($p < 0.001$).

For DistMaxtoIpsiT, the two-way repeated measures ANOVA revealed no significant interaction effect between TMS Intensity and forward-bending angle [F(4, 152) = 0.559; $p = 0.693$; $\eta_p^2 = 0.015$]. The main effect of TMS Intensity [F(2, 152) = 1.945; $p = 0.147$; $\eta_p^2 = 0.025$] and forward-bending angle [F(2, 152) = 1.930; $p = 0.149$; $\eta_p^2 = 0.025$] were both not significant.

For DistMaxtoContraT, the two-way repeated measures ANOVA revealed no significant interaction effect between TMS Intensity and forward-bending angle [F(4, 152) = 0.490; $p = 0.743$; $\eta_p^2 = 0.013$] and no main effect of TMS Intensity [F(2, 152) = 0.171; $p = 0.843$; $\eta_p^2 = 0.002$]. The main effect of forward-bending angle was significant [F(2, 152) = 5.564; $p = 0.005$; $\eta_p^2 = 0.068$]. For factor of forward-bending angle, post-hoc comparisons showed that DistMaxtoContraT during 0 degree of forward-bending angle was significantly larger than that during 30 degree of forward-bending angle ($p = 0.031$) and that during 60 degree of forward-bending angle ($p = 0.007$).

C. Comparison of Feature Parameters of MEP Topographic Maps in Different Sides

With shown in the Fig. 7, the amplitude of MEP in the target spot and the distance between the target spot and Max spot were different between the ipsilateral and contralateral side.

By using independent T test, the amplitude of MEP in the IpsiT spot was significantly larger than that in the ContraT spot during some TMS intensity and forward-bending angle (60% of MSO and 0 degree of forward-bending angle: $p < 0.01$; 80% of MSO and 0 degree of forward-bending angle: $p < 0.01$; 80% of MSO and 30 degree of forward-bending angle: $p < 0.05$; 80% of MSO and 60 degree of forward-bending angle: $p < 0.01$). Similarly, the distance from the Max spot to the IpsiT spot was significantly smaller ($p < 0.01$) than the one from the Max spot to the ContraT spot during all different TMS intensity and forward-bending angle.

IV. Discussion

In this study, by analyzing the high-density sEMG signals from the surface of lumbar paravertebral muscles, the MEP topographic map elicited by single-pulse TMS could be obtained. TMS could successfully evoke an oval area with high intensity in the MEP topographic map, while this area mainly located in the ipsilateral side of the TMS site. Intensity features related to the high intensity area rose significantly with TMS intensity and forward-bending angle increasing, but location features showed no change. The high intensity area in this map can accurately indicate the effect of transcranial stimulation on trunk muscles.

In the MEP topographic map, there appeared a high intensity area. The shape of this area tended to be like an oval. This oval area had a central spot which showed the largest amplitude of MEP. This finding is similar with previous studies on the MEP topographic map from extremity muscles [16]–[18]. They used the high-density sEMG to investigated the spatial distribution of MEPs in the forearm extensors. For one type of forearm muscle such as extensor carpi radialis, the color maps of the spatial distribution displayed a high intensity area. Displayed in the quantitative analysis, there was no statistically significant difference on the relative area and the distance from the Max spot to the target spot among different TMS parameters. It indicated the TMS site and the elicited spot of trunk muscles was precisely correlated. By using the MEP topographic map, it is potential to find out the hotspot for the TMS on cortex related to the trunk muscles.

In this study, it is obvious that the amplitude of MEP in the MEP topographic map from trunk muscles is related to the TMS intensity and forward-bending angle. It increased as the TMS intensity increased or the forward-bending angle increased. It is consistent with previous findings that the TMS intensity and muscle activity were important factors for MEPs [32], [33]. For factor of TMS intensity, a higher TMS intensity could lead to a stronger magnetic field which activated a larger proportion of corticospinal neurons [32], [33]. The D-waves and I-waves might be induced by direct activation of the axon hillock, so as to activate more muscle fibers [34]. For factor of muscle activity, a larger bending angle could result in a larger muscle activity [percentage of maximal voluntary contraction (MVC)]. When comparing a resting and slightly active muscle, previous studies showed increased muscle activity was mainly attributed to changes in excitability at the spinal level [32]. A greater cortical area was sensitive to eliciting a MEP when the muscle was active [35]. Consequently, as forward-bending angle increased, the corticospinal pathway became more and more sensitive to the activation on the cortical area.

Furthermore, because the motor threshold during active contraction of the target muscle, also named the active motor threshold (AMT), which is considered an indicator of cortical excitability, is often defined as the minimum intensity required to elicit $>200\mu$V MEP in 5/10 consecutive trials [36], our findings indicated the MEP during 30 or 60 degree of forward-bending angle was more likely to meet the requirements. For the optimal TMS intensity to elicit MEP topographic map of trunk muscles, 80% of MSO was more appropriate, according to the Fig. 7a. Therefore, among the TMS parameters (TMS intensity: 60%, 80%, 100% of MSO; Forward-bending angle: 0 degree, 30 degree, 60 degree), 80% of MSO and 30 or 60 degree of forward-bending angle are the optimal TMS parameters to construct MEP topographic map of trunk muscles.

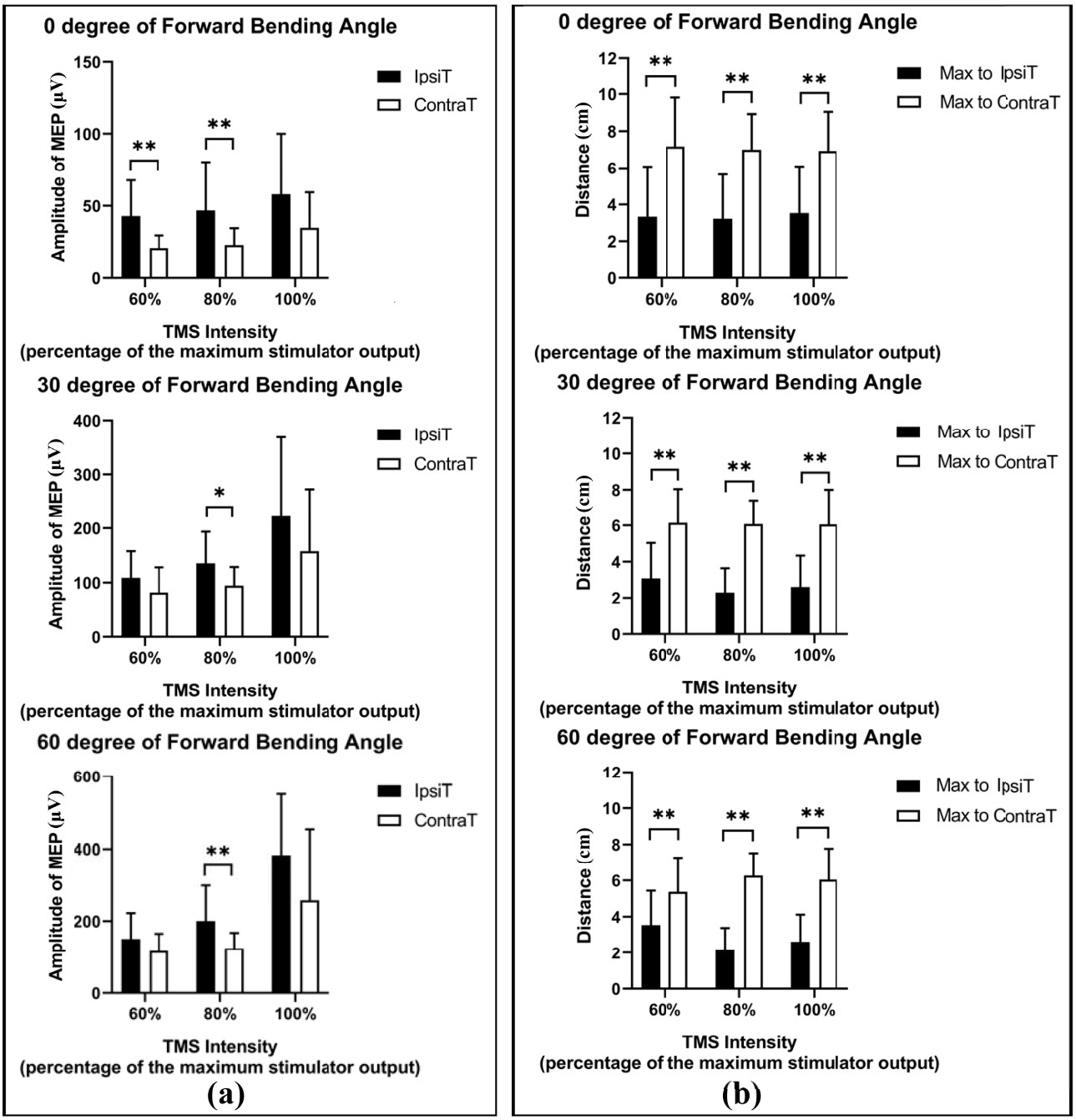

Fig. 7. Comparison of features between ipsilateral-side stimulation and contralateral-side stimulation. IpsiT means the target muscle spot in the ipsilateral side of the TMS site, while ContraT means the target muscle spot in the contralateral side of the TMS site. Max means the muscle spot with the maximum amplitude value of MEP. The unit of amplitude of MEP is μV while the unit of Distance is cm. (A) Amplitude of MEP in target muscle spot during different forward-bending angle; (B) Distance from Max muscle spot to target muscle spot during different forward-bending angle. * indicates $p < 0.05$. ** indicates $p < 0.01$.

No matter in qualitative or quantitative analysis results, the high intensity area in most MEP topographic map located ipsilaterally compared with the TMS site. This finding interestingly indicates that the corticospinal projection from transcranial stimulation site to trunk muscles is different with that to extremity muscle. Some previous studies also found unilateral TMS at the primary motor cortex could produce ipsilateral excitatory responses in both right and left erector spinae [37]. This ipsilateral MEP could only be evoked in the axial muscles (erector spinae) rather than in the arm muscles (anterior deltoid and first dorsal interosseous) [7]. The reason why these findings are obtained may be due to the neural pathway from motor cortex to trunk muscles. The bilaterally organized neural pathway such as corticoreticulospinal or propriospinal pathway had been verified to mediate ipsilateral excitatory responses [38]. The study on primate and mice showed a corticoreticulospinal pathway from supplementary motor area (SMA) to cervical cord via the reticulospinal system did exist [39]. The existence

of descending axons (dCINs) in the lumbar spinal cord could mediate responses in lumbar motoneurons via reticulospinal pathways originating from the medial and lateral medullary reticular formation (MRF) [40]. This pathway showed the capacity to influence both the ipsilateral and contralateral trunk musculature [39], [40]. Therefore, the bilaterally neural pathway from motor cortex to trunk muscles may account for the finding of ipsilateral high intensity area in the MEP topographic map in this study.

There are also several limitations in this study. Firstly, the hotspot for lumbar paravertebral muscles from our findings was different with that in the previous studies (1 cm anterior and 4 cm lateral to the vertex). In previous studies [5], [13], [14], when stimulating the hotspot (1 cm anterior and 4 cm lateral to the vertex), the MEP signal from the spot 3 cm lateral to the L3 spinous process (central spot in the topographic map) showed the most response. In this study, when we stimulated the same hotspot, the Max muscle spot showed difference. For all participants' map data, the distance from the Max muscle spot to the target muscle spot (3 cm lateral to the L3 spinous process) was not even close to zero. It might due to the characteristics of instability for TMS-evoked MEPs or the inaccurate hotspot in previous studies. It will be investigated in the future. Secondly, the TMS-related activity of cortical area is missing. It will help to explore the role of the cortex in the corticospinal projection to trunk muscles. The TMS-evoked Electroencephalography (EEG) will be collected synchronously in the future. Thirdly, further investigations of the proposed method in this study will be carried on the patients with muscular disorders to verify its clinical effectiveness.

V. Conclusion

In summary of this study, by using high-density sEMG electrodes, we collected the MEPs from lumber paravertebral muscles and constructed the MEP topographic map. With this map, the proportion of lumbar paravertebral muscles affected by TMS showed relation with the TMS intensity and forward-bending angle. Among the TMS parameters (TMS intensity: 60%, 80%, 100% of MSO; Forward-bending angle: 0 degree, 30 degree, 60 degree), the optimal stimulation parameters were 80% of MSO for TMS intensity and 30/60 degree for forward-bending angle. This study may provide a potential effective mapping tool to explore the hotspot for transcranial stimulation on lumbar paravertebral muscles.

References

[1] K. Pacheco-Barrios, X. Meng, and F. Fregni, "Neuromodulation techniques in phantom limb pain: A systematic review and meta-analysis," *Pain Med.*, vol. 21, no. 10, pp. 2310–2322, Oct. 2020.

[2] K. Hosomi *et al.*, "A randomized controlled trial of 5 daily sessions and continuous trial of 4 weekly sessions of repetitive transcranial magnetic stimulation for neuropathic pain," *Pain*, vol. 161, no. 2, pp. 351–360, Feb. 2020.

[3] N. Jiang, J. Wei, G. Li, B. Wei, F. F. Zhu, and Y. Hu, "Effect of dry-electrode-based transcranial direct current stimulation on chronic low back pain and low back muscle activities: A double-blind sham-controlled study," *Restorative Neurol. Neurosci.*, vol. 38, no. 1, pp. 41–54, Feb. 2020.

[4] N. E. O'Connell *et al.*, "Transcranial direct current stimulation of the motor cortex in the treatment of chronic nonspecific low back pain: A randomized, double-blind exploratory study," *Clin. J. Pain*, vol. 29, no. 1, pp. 26–34, Jan. 2013.

[5] S. M. Schabrun, E. Jones, E. L. Elgueta Cancino, and P. W. Hodges, "Targeting chronic recurrent low back pain from the top-down and the bottom-up: A combined transcranial direct current stimulation and peripheral electrical stimulation intervention," *Brain Stimulation*, vol. 7, no. 3, pp. 451–459, May 2014.

[6] N. Jiang, G. Li, J. Wei, B. Wei, F. F. Zhu, and Y. Hu, "Transcranial direct current stimulation of the primary motor cortex on postoperative pain and spontaneous oscillatory electroencephalographic activity following lumbar spine surgery: A pilot study," *Restor. Neurol. Neurosci.*, vol. 36, pp. 605–620, Sep. 2018.

[7] L. Jean-Charles, J.-F. Nepveu, J. E. Deffeyes, G. Elgbeili, N. Dancause, and D. Barthélemy, "Interhemispheric interactions between trunk muscle representations of the primary motor cortex," *J. Neurophysiol.*, vol. 118, no. 3, pp. 1488–1500, Sep. 2017.

[8] H. Tsao, K. J. Tucker, and P. W. Hodges, "Changes in excitability of corticomotor inputs to the trunk muscles during experimentally-induced acute low back pain," *Neuroscience*, vol. 181, pp. 127–133, May 2011.

[9] S.-Y. Chiou, S. E. A. Gottardi, P. W. Hodges, and P. H. Strutton, "Corticospinal excitability of trunk muscles during different postural tasks," *PLoS ONE*, vol. 11, no. 1, Jan. 2016, Art. no. e0147650.

[10] F. Behrendt, M. H. E. de Lussanet, K. Zentgraf, and V. R. Zschorlich, "Motor-evoked potentials in the lower back are modulated by visual perception of lifted weight," *PLoS ONE*, vol. 11, no. 6, Jun. 2016, Art. no. e0157811.

[11] B. C. Clark, D. A. Goss, S. Walkowski, R. L. Hoffman, A. Ross, and J. S. Thomas, "Neurophysiologic effects of spinal manipulation in patients with chronic low back pain," *BMC Musculoskeletal Disorders*, vol. 12, no. 1, p. 170, Jul. 2011.

[12] S. M. Schabrun, E. L. Elgueta-Cancino, and P. W. Hodges, "Smudging of the motor cortex is related to the severity of low back pain," *Spine*, vol. 42, no. 15, pp. 1172–1178, Aug. 2017.

[13] N. E. O'Connell, D. W. Maskill, J. Cossar, and A. V. Nowicky, "Mapping the cortical representation of the lumbar paravertebral muscles," *Clin. Neurophysiol.*, vol. 118, no. 11, pp. 2451–2455, Nov. 2007.

[14] H. Tsao, L. Danneels, and P. W. Hodges, "Individual fascicles of the paraspinal muscles are activated by discrete cortical networks in humans," *Clin. Neurophysiol.*, vol. 122, no. 8, pp. 1580–1587, Aug. 2011.

[15] A. Bastani and S. Jaberzadeh, "A-tDCS differential modulation of corticospinal excitability: The effects of electrode size," *Brain Stimulation*, vol. 6, no. 6, pp. 932–937, Nov. 2013.

[16] J. L. Neva, A. Gallina, S. Peters, S. J. Garland, and L. A. Boyd, "Differentiation of motor evoked potentials elicited from multiple forearm muscles: An investigation with high-density surface electromyography," *Brain Res.*, vol. 1676, pp. 91–99, Dec. 2017.

[17] G. van Elswijk, B. U. Kleine, S. Overeem, B. Eshuis, K. D. Hekkert, and D. F. Stegeman, "Muscle imaging: Mapping responses to transcranial magnetic stimulation with high-density surface electromyography," *Cortex*, vol. 44, no. 5, pp. 609–616, May 2008.

[18] A. Gallina, S. Peters, J. L. Neva, L. A. Boyd, and S. J. Garland, "Selectivity of conventional electrodes for recording motor evoked potentials: An investigation with high-density surface electromyography," *Muscle Nerve*, vol. 55, no. 6, pp. 828–834, Jun. 2017.

[19] Y. Hu, S. H. Siu, J. N. Mak, and K. D. Luk, "Lumbar muscle electromyographic dynamic topography during flexion-extension," *J. Electromyogr. Kinesiol.*, vol. 20, no. 2, pp. 246–255, Apr. 2010.

[20] A. Liu, Z. J. Wang, and Y. Hu, "Network modeling and analysis of lumbar muscle surface EMG signals during flexion–extension in individuals with and without low back pain," *J. Electromyogr. Kinesiol.*, vol. 21, no. 6, pp. 913–921, Dec. 2011.

[21] N. Jiang, J. Xue, and G. Li, "Assessment of lumbar muscles coordinated activity based on high-density surface electromyography: A pilot study," in *Proc. 41st Annu. Int. Conf. IEEE Eng. Med. Biol. Soc. (EMBC)*, Jul. 2019, pp. 2238–2241.

[22] N. Jiang, K. D.-K. Luk, and Y. Hu, "A machine learning-based surface electromyography topography evaluation for prognostic prediction of functional restoration rehabilitation in chronic low back pain," *Spine*, vol. 42, no. 21, pp. 1635–1642, Nov. 2017.

[23] Y. Hu, J. W. Kwok, J. Y.-H. Tse, and K. D.-K. Luk, "Time-varying surface electromyography topography as a prognostic tool for chronic low back pain rehabilitation," *Spine J.*, vol. 14, no. 6, pp. 1049–1056, Jun. 2014.

[24] Y. Jinglin, H.-X. Li, and H. Yong, "A probabilistic SVM based decision system for pain diagnosis," *Expert Syst. Appl.*, vol. 38, no. 8, pp. 9346–9351, Aug. 2011.
[25] Y.-L. Huang *et al.*, "Assessment of lumbar paraspinal muscle activation using fMRI BOLD imaging and T2 mapping," *Quant. Imag. Med. Surgery*, vol. 10, no. 1, pp. 106–115, Jan. 2020.
[26] J. D. Dishman, K. A. Ball, and J. Burke, "First prize central motor excitability changes after spinal manipulation: A transcranial magnetic stimulation study," *J. Manipulative Physiol. Therapeutics*, vol. 25, no. 1, pp. 1–9, Jan. 2002.
[27] H. Tsao, M. P. Galea, and P. W. Hodges, "Concurrent excitation of the opposite motor cortex during transcranial magnetic stimulation to activate the abdominal muscles," *J. Neurosci. Methods*, vol. 171, no. 1, pp. 132–139, Jun. 2008.
[28] M. Brum, C. Cabib, and J. Valls-Solé, "Clinical value of the assessment of changes in MEP duration with voluntary contraction," *Front Neurosci.*, vol. 9, p. 505, Jan. 2016.
[29] C. Neige, S. Grosprátre, A. Martin, and F. Lebon, "Influence of voluntary contraction level, test stimulus intensity and normalization procedures on the evaluation of short-interval intracortical inhibition," *Brain Sci.*, vol. 10, no. 7, p. 433, Jul. 2020.
[30] J. Dvoák, M. M. Panjabi, D. G. Chang, R. Theiler, and D. Grob, "Functional radiographic diagnosis of the lumbar spine: Flexion—extension and lateral bending," *Spine*, vol. 16, no. 5, pp. 562–571, May 1991.
[31] A. du Rose and A. Breen, "Relationships between paraspinal muscle activity and lumbar inter-vertebral range of motion," *Healthcare*, vol. 4, no. 1, p. 4, Jan. 2016.
[32] M. van de Ruit and M. J. Grey, "The TMS map scales with increased stimulation intensity and muscle activation," *Brain Topography*, vol. 29, no. 1, pp. 56–66, Jan. 2016.
[33] J. Grandjean, G. Derosiere, P. Vassiliadis, L. Quemener, Y. D. Wilde, and J. Duque, "Towards assessing corticospinal excitability bilaterally: Validation of a double-coil TMS method," *J. Neurosci. Methods*, vol. 293, pp. 162–168, Jan. 2018.
[34] V. Di Lazzaro *et al.*, "Corticospinal volleys evoked by transcranial stimulation of the brain in conscious humans," *Neurol. Res.*, vol. 25, no. 2, pp. 143–150, Mar. 2003.
[35] E. M. Wassermann, "Variation in the response to transcranial magnetic brain stimulation in the general population," *Clin. Neurophysiol.*, vol. 113, no. 7, pp. 1165–1171, Jul. 2002.
[36] E. Zewdie, O. Damji, P. Ciechanski, T. Seeger, and A. Kirton, "Contralesional corticomotor neurophysiology in hemiparetic children with perinatal stroke," *Neurorehabil. Neural Repair*, vol. 31, no. 3, pp. 261–271, Mar. 2017.
[37] A. Kuppuswamy, M. Catley, N. K. King, P. H. Strutton, N. J. Davey, and P. H. Ellaway, "Cortical control of erector spinae muscles during arm abduction in humans," *Gait Posture*, vol. 27, no. 3, pp. 478–484, Apr. 2008.
[38] U. Ziemann *et al.*, "Dissociation of the pathways mediating ipsilateral and contralateral motor-evoked potentials in human hand and arm muscles," *J. Physiol.*, vol. 518, no. 3, pp. 895–906, Aug. 1999.
[39] L. R. Montgomery, "Role of the reticulospinal and corticoreticular systems for the control of reaching in non human primates," Ph.D. dissertation, Graduate School, Ohio State Univ., Columbus, OH, USA, 2013.
[40] K. Szokol, J. C. Glover, and M.-C. Perreault, "Organization of functional synaptic connections between medullary reticulospinal neurons and lumbar descending commissural interneurons in the neonatal mouse," *J. Neurosci.*, vol. 31, no. 12, pp. 4731–4742, Mar. 2011.